



Scholars Research Library

Der Pharma Chemica, 2014, 6(4):373-379  
(<http://derpharmachemica.com/archive.html>)



ISSN 0975-413X  
CODEN (USA): PCHHAX

## On the electrophilic reactivities of $\alpha$ -carbonyl heterocycles and arenes

Jeffrey L. Wells and Douglas A. Klumpp\*

Department of Chemistry, Northern Illinois University, DeKalb, Illinois

---

### ABSTRACT

A series of heterocyclic aldehydes and substituted benzaldehydes were studied for their tendencies to form hemi-acetal products with methanol. The equilibrium ratios were compared with DFT calculated molecular orbital levels and the hemi-acetal content was found to correlate roughly to the energy level of the lowest unoccupied molecular orbitals (LUMOs). Hemi-acetal formation is enhanced by intramolecular hydrogen bonds and diminished by steric effects.

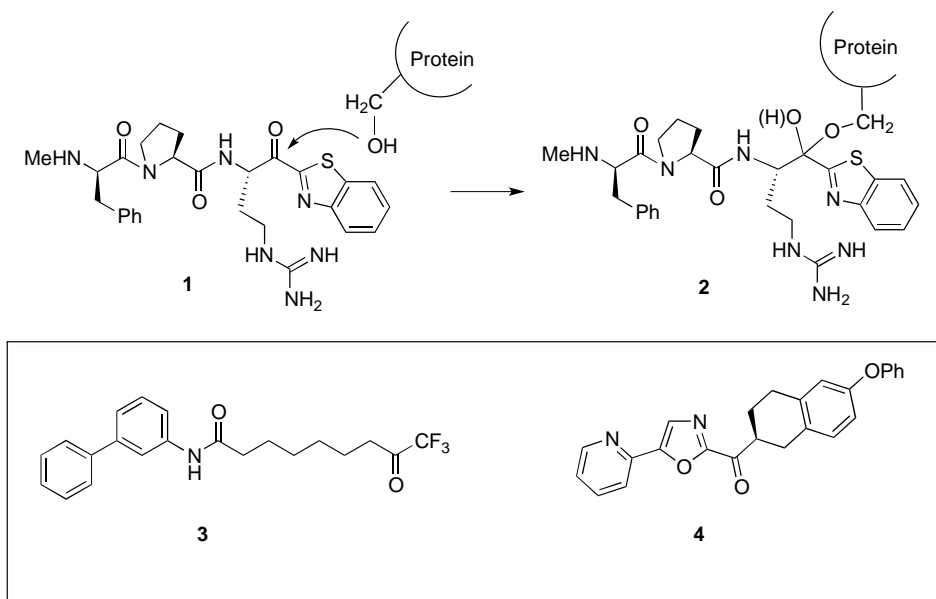
**Keywords:** electrophilic, heterocycles, hemi-acetal, carbonyl

---

### INTRODUCTION

Electrophilic aldehydes and ketones have long been recognized as potentially useful agonist and antagonist compounds in therapeutic applications.<sup>1</sup> Such compounds often have the ability to form covalent adducts with nucleophilic functional groups at receptor sites. For example, electrophilic aldehydes and ketones have been shown to inhibit serine proteases and this biological activity usually occurs by formation of hemi-acetal adducts (Scheme 1).<sup>2-4</sup> In the case of compound **1** (a potent thrombin inhibitor), reaction of the serine residue leads to formation of the hemi-acetal covalent complex **2** and inhibition of the protein.<sup>2</sup> Other examples of electrophilic ketones include Abbott's histone deacetylase inhibitor<sup>3</sup> (**3**) and Boger's FAAH inhibitor<sup>4</sup> (**4**). The heterocyclic and trifluoromethyl ketones are effective enzyme inhibitors largely due to the highly electrophilic carbonyl groups on these compounds – an effect caused by the strong electron withdrawing abilities of the heterocyclic rings and the trifluoromethyl group.

According to the frontier molecular orbital theory, electrophilic reactivity is controlled by the energy levels of the lowest unoccupied molecular orbital (LUMO) on the electrophile and the highest occupied molecular orbital (HOMO) on the nucleophile.<sup>5</sup> Enzyme inhibitors such as **1**, **3**, and **4** are characterized by relatively low energy LUMOs at the carbonyl group and therefore they are reactive electrophilic compounds. While it is understood that low energy LUMOs can be related to high electrophilic reactivities, it could be extremely useful if LUMO energy levels could be correlated to hemi-acetal content for electrophilic carbonyl groups. This information would be useful to medicinal chemists as prospective drugs could be studied computationally to determine molecular orbital energies and their electrophilic reactivities could be predicted. In the following manuscript, we describe our studies of a series of heterocyclic aldehydes and substituted benzaldehydes and their tendencies to form hemi-acetal products with methanol. The equilibrium mixtures are also compared with LUMO energy levels for the aldehydes. Besides demonstrating a correlation between LUMO energies and hemi-acetal content, we also found evidence for structural features that may favor hemi-acetal formation.



Scheme 1. Hemi-acetal formation with thrombin inhibitor 1 and other electrophilic enzyme inhibitors (3-4)

### MATERIALS AND METHODS

For the aldehydes in this study, hemi-acetal content was measured using  $^1\text{H}$  NMR spectroscopy. The aldehyde was dissolved in  $\text{CD}_3\text{OD}$  and allowed to equilibrate for 1 hr. at  $25^\circ\text{C}$  and then the  $^1\text{H}$  NMR spectrum was taken. The aldehyde/hemi-acetal ratio was conveniently measured by integration of the aldehyde proton ( $\delta$  9-10) and hemiacetalmethineproton ( $\delta$  5-6) in the  $^1\text{H}$  NMR spectrum (Figure 1). It was assumed that deuterium isotope effects – if any – would be similar between the various aldehydes. The mixtures were analyzed by  $^{13}\text{C}$  NMR to verify the formation of hemi-acetal products. We also compared the  $^1\text{H}$  NMR spectra from methanol with spectra of the pure aldehydes in  $\text{CDCl}_3$ . Although the conversion between aldehyde and hemi-acetal involves some proton transfer steps in the mechanism, no intermediates were observed in the NMR studies. Theoretical calculations were done to determine the energy levels of the molecular orbitals for each aldehyde.<sup>6</sup> Geometry optimizations were done using density function theory and the hybrid functional B3LYP at the 6-311G\*\* level.<sup>7,8</sup> Vibrational analyses were performed at the B3LYP/6-311G\*\* level of theory and all optimized structures were found to have zero imaginary frequencies.

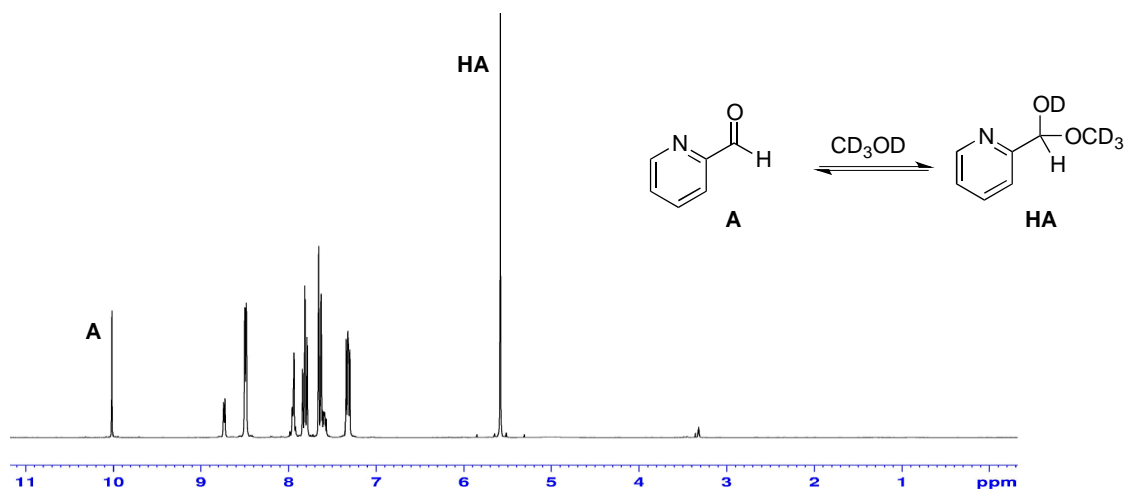
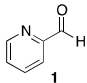
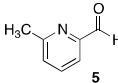
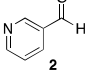
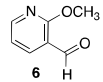
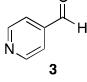
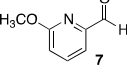
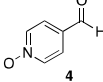
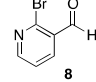


Figure 1. The  $^1\text{H}$  NMR spectrum of a mixture of 2-pyridinecarboxaldehyde (A) and the hemi-acetal (HA) product in  $\text{CD}_3\text{OD}$

## RESULTS

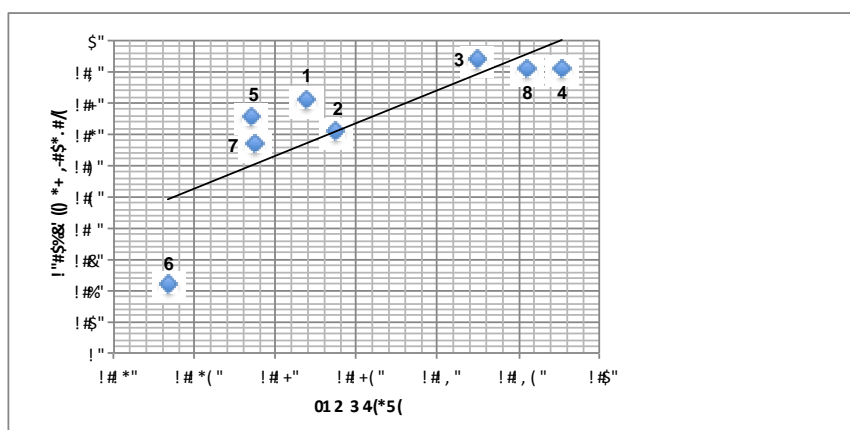
Our first group of experiments examined a series of pyridine carboxaldehydes. This series was chosen because of the electron withdrawing properties of the pyridine ring, the use of this heterocycle in many pharmaceutical agents, and the availability of pyridinecarboxaldehydes. The isomeric pyridinecarboxaldehydes (**1-3**), substituted derivatives (**5-8**), and the pyridine *N*-oxide (**4**), were all dissolved in CD<sub>3</sub>OD and analyzed by <sup>1</sup>H NMR for the hemi-acetal content (Table 1). These same aldehydes were studied using DFT calculations and the LUMO energy levels estimated. In general, hemi-acetal content correlated reasonably well with the LUMO level – the more highly negative LUMOs are increasingly electrophilic (Chart 1). Most of the pyridinecarboxaldehydes followed this trend, although 2-methoxy-3-pyridinecarboxaldehyde (**6**) formed less than the expected amount of hemi-acetal. This may be due to the resonance interactions of the methoxy group with aldehyde group (decreasing its electrophilic reactivity), or it may be due to the steric demands of the hemi-acetal functional group. Interestingly, the pyridine *N*-oxide (**4**) exhibits a low energy LUMO and consequently a high degree of hemi-acetal formation (0.91). Its electrophilic properties are nearly identical to 4-pyridinecarboxaldehyde (**3**), yet the basicity of compound **4** is significantly less than **3** (at the ring).<sup>9</sup> We also treated each of the pyridinecarboxaldehydes with 1.0 equivalents of methanesulfonic acid and the resulting pyridinium salts were all completely converted to the hemi-acetals in CD<sub>3</sub>OD.

Table 1. Pyridinecarboxaldehyde derivative (**1-8**), their calculated LUMO levels, and the fraction of hemi-acetal formation in CD<sub>3</sub>OD

Aldehyde	LUMO <sup>a</sup>	Fraction Hemi-Acetal <sup>b</sup>	Aldehyde	LUMO <sup>a</sup>	Fraction Hemi-Acetal <sup>b</sup>
	-0.08189 eV	0.81		-0.07852 eV	0.76
	-0.08372 eV	0.71		-0.07331 eV	0.22
	-0.09242 eV	0.94		-0.07867 eV	0.67
	-0.09767 eV	0.91		-0.09554 eV	0.91

<sup>a</sup>Calculated at the B3LYP 6-311G\*\* level. <sup>b</sup>Measured by <sup>1</sup>H NMR and calculated as [hemi-acetal]/[hemi-acetal + aldehyde]

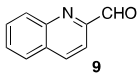
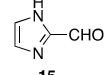
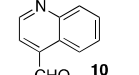
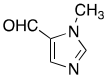
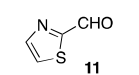
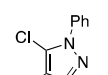
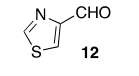
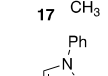
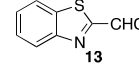
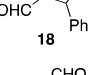
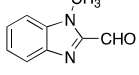
Chart 1. Pyridinecarboxaldehydes and LUMO energies



In addition to the pyridines, we studied a variety of heterocyclic aldehydes (Table 2 and Chart 2). The highest energy LUMOs were found with the imidazole (**15-16**) and the pyrazolecarboxaldehydes (**17-18**), while the lowest

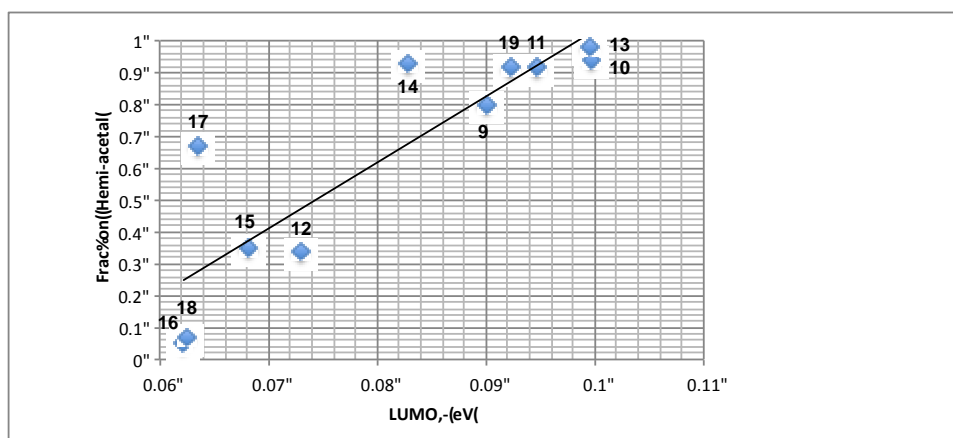
energy LUMOs were found with the quinolone (**10**) and benzothiazole (**13**) carboxaldehydes. As expected, the high energy LUMOs are associated with the lowest fraction of hemi-acetal content and the low energy LUMOs are associated with a large degree of hemi-acetal formation. When the LUMO energies and hemi-acetal content are compared, there is a clear correlation between the two parameters (Chart 2), though some scatter can be seen with aldehydes **14** and **17**. The correlation reasonably good, especially considering the variety of heterocycles examined. Compound **17** forms a remarkable amount of hemi-acetal considering the energy level of its LUMO. This observation may be due to hydrogen bonding between the hemi-acetal group and the adjacent chlorine substituent (eq 1). The hydrogen bonding stabilizes the hemi-acetal and tends to favor its formation.

**Table 2. Heterocyclic derivative (9-19), their calculated LUMO levels, and the fraction of hemi-acetal formation in CD<sub>3</sub>OD**

Aldehyde	LUMO <sup>a</sup>	Fraction Hemi-Acetal <sup>b</sup>	Aldehyde	LUMO <sup>a</sup>	Fraction Hemi-Acetal <sup>b</sup>
	-0.08999 eV	0.80		-0.06810 eV	0.35
	-0.09973 eV	0.94		-0.06220 eV	0.05
	-0.09472 eV	0.92		-0.06354 eV	0.67
	-0.07297 eV	0.34		-0.06249 eV	0.07
	-0.09947 eV	0.98		-0.09229 eV	0.92
	-0.08280 eV	0.93			

<sup>a</sup>Calculated at the B3LYP 6-311G\*\* level. <sup>b</sup>Measured by <sup>1</sup>H NMR and calculated as [hemi-acetal]/[hemi-acetal + aldehyde]

**Chart 2. Heterocyclic carboxaldehyde hemi-acetals and LUMO energies**



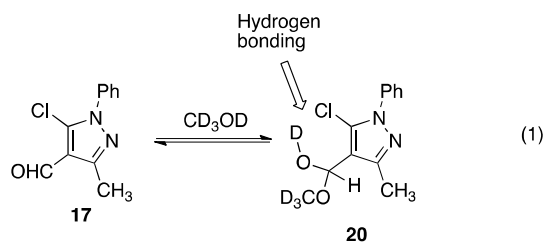
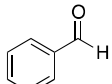
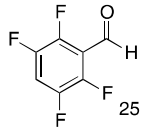
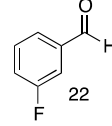
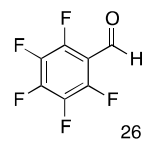
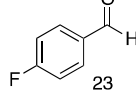
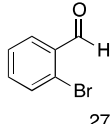
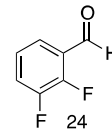
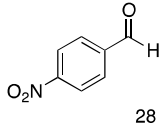


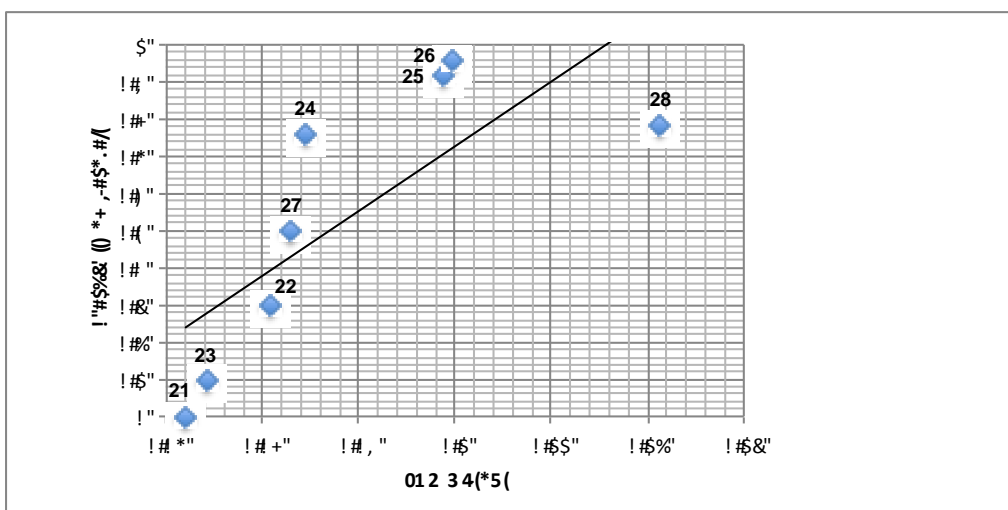
Table 3. Benzaldehyde derivative (21-28), their calculated LUMO levels, and the fraction of hemi-acetal formation in CD<sub>3</sub>OD

Aldehyde	LUMO <sup>a</sup>	Fraction Hemi-Acetal <sup>b</sup>	Aldehyde	LUMO <sup>a</sup>	Fraction Hemi-Acetal <sup>b</sup>
 21	-0.07197 eV	~0.00	 25	-0.09866 eV	0.92
 22	-0.08080 eV	0.30	 26	-0.09966 eV	0.96
 23	-0.07420 eV	0.10	 27	-0.08439 eV	0.50
 24	-0.08439 eV	0.76	 28	-0.12132 eV	0.78

<sup>a</sup>Calculated at the B3LYP 6-311G\*\* level.

<sup>b</sup>Measured by <sup>1</sup>H NMR and calculated as [hemi-acetal]/[hemi-acetal + aldehyde]

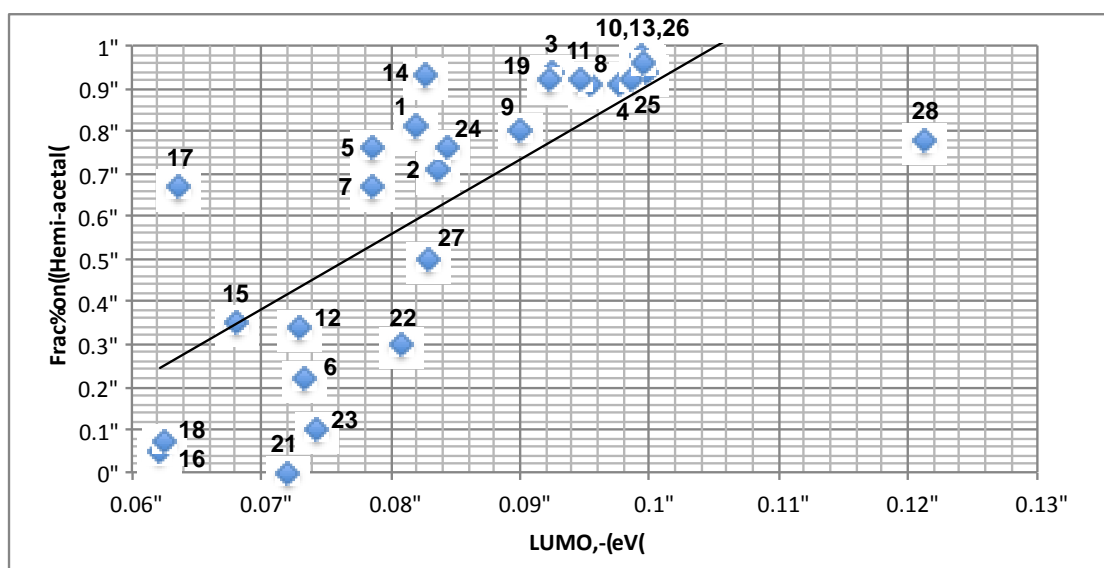
Chart 3. Benzaldehyde hemi-acetals and LUMO energies



Finally, a series of benzaldehydes were also examined. In general, the content of hemi-acetal increases with the lowered LUMOs (Table 3). Nevertheless, the plot of LUMO energies and hemi-acetal content does show considerable amount of scatter (Chart 3). Most notably, 4-nitrobenzaldehyde (**28**) shows a surprisingly low amount of hemi-acetal content (0.78) considering it possesses the lowest LUMO in the series. Another interpretation could invoke hydrogen bonding with compounds **24-27**, all of which could form hemi-acetal products capable of intramolecular hydrogen-bonding. This should elevate the amount of hemi-acetal relative to aldehydes **21-23** and **28** (none of which could form the hydrogen-bond stabilized hemi-acetal). It should also be noted that initial experiments with benzaldehyde showed large amounts of the hemi-acetal along with some acetal product. These products are assumed to form by rapid, acid-catalyzed processes in the excess CD<sub>3</sub>OD solvent. Evidently, the benzaldehyde contained catalytic amounts of benzoic acid. If the benzaldehyde is purified or the reaction is run with an equivalent of pyridine, then very little of the hemi-acetal is observed (Table 3).

Finally, all three sets of data were combined for comparison (Chart 4). Although the plot exhibits scatter, there is clearly a relationship between LUMO energies and the extent of hemi-acetal formation, even between widely varying structure types. Without exception, aldehydes having LUMO energies lower than -0.09 eV exist primarily (>80%) as the hemi-acetal in CD<sub>3</sub>OD. This is likely due to the high electrophilic reactivity associated with the low energy LUMO. Other effects clearly influence the position of these equilibria and presumably these additional factors contribute to the scatter of the plot. As previously noted, intramolecular hydrogen bonding may be causing the large amount of hemi-acetal in the case of pyrazole **17**. Steric effects, solvation, charge distributions, and acid-base properties (of the aldehyde/hemi-acetals) may also be influencing the position of the equilibria.

Chart 4. Combined plot of all aldehydes (1-19, 21-28) and LUMO energies



## CONCLUSION

We have found that calculated LUMO levels of aldehydes correlate reasonably well with their tendency to form hemi-acetal products with methanol. In one case, the results suggested that intramolecular hydrogen bonding can favor hemi-acetal formation.

## Acknowledgement

The financial support from the NIH-National Institute of General Medical Sciences (GM085736-01A1) is gratefully acknowledged.

## REFERENCES

- [1] B. E. Maryanoff; M. J. Costanzo *Bioorg. Med. Chem.* **2008**, *16*, 1562.
- [2] M. J. Costanzo; H. R. Almond, Jr.; L. R. Hecker; M. R. Schott; S. C. Yabut; H.-C. Zhang; P. Andrade-Gordon; T. W. Concoran; E. C. Giardino; J. A. Kauffman; J. M. Lewis; L. de Garavilla; B. J. Haertlein; B. E. Maryanoff *J. Med. Chem.* **2005**, *48*, 1984.
- [3] R. R. Frey; C. K. Wada; R. B. Garland; M. L. Curtin; M. R. Michaelides; J. Li; L. J. Pease; K. B. Glaser; P. A. Marcotte; J. J. Bouska; S. S. Murphy; S. K. Davidsen *Bioorg. Med. Chem. Lett.* **2002**, *12*, 3443.
- [4] K. Otrubova; D. L. Boger *ACS Chem. Neuro.* **2012**, *3*, 340.
- [5] a. K. Fukui *Angew. Chem. Int. Ed.* **2003**, *21*, 801. b. G. Klopman *J. Am. Chem. Soc.* **1968**, *90*, 223.
- [6] Gaussian 09, Revision B.01, M. J. Frisch, G. W. Trucks, H. B. Schlegel, G. E. Scuseria, M. A. Robb, J. R. Cheeseman, G. Scalmani, V. Barone, B. Mennucci, G. A. Petersson, H. Nakatsuji, M. Caricato, X. Li, H. P. Hratchian, A. F. Izmaylov, J. Bloino, G. Zheng, J. L. Sonnenberg, M. Hada, M. Ehara, K. Toyota, R. Fukuda, J. Hasegawa, M. Ishida, T. Nakajima, Y. Honda, O. Kitao, H. Nakai, T. Vreven, J. A. Montgomery, Jr., J. E. Peralta, F. Ogliaro, M. Bearpark, J. J. Heyd, E. Brothers, K. N. Kudin, V. N. Staroverov, R. Kobayashi, J. Normand, K. Raghavachari, A. Rendell, J. C. Burant, S. S. Iyengar, J. Tomasi, M. Cossi, N. Rega, J. M. Millam, M. Klene, J. E. Knox, J. B. Cross, V. Bakken, C. Adamo, J. Jaramillo, R. Gomperts, R. E. Stratmann, O. Yazyev, A. J. Austin, R. Cammi, C. Pomelli, J. W. Ochterski, R. L. Martin, K. Morokuma, V. G. Zakrzewski, G. A. Voth, P. Salvador, J. J. Dannenberg, S. Dapprich, A. D. Daniels, Ö. Farkas, J. B. Foresman, J. V. Ortiz, J. Cioslowski, and D. J. Fox, Gaussian, Inc., Wallingford CT, **2009**.
- [7] (a) A. D. Becke *Phys. Rev. A* **1988**, *38*, 3098. (b) A. D. Becke *J. Chem. Phys.* **1993**, *98*, 5648. (c) C. Lee; W. Yang; R. G. Parr *Phys. Rev. B* **1988**, *37*, 785.
- [8] K. Raghavachari; J. S. Binkley; R. Seegar; J. A. Pople *J. Chem. Phys.* **1980**, *72*, 650.
- [9] H. H. Jaffe; G. O. Doak *J. Am. Chem. Soc.* **1955**, *77*, 4441.